

An acetylation–mono-ubiquitination switch on lysine 120 of H2B

Raffaella Gatta,¹ Diletta Dolfini,¹ Federico Zambelli,¹ Carol Imbriano,² Giulio Pavesi¹ and Roberto Mantovani^{1,*}

¹Dipartimento di Scienze Biomolecolari e Biotecnologie; Università degli Studi di Milano; Milano, Italy; ²Dipartimento di Biologia Animale; Università di Modena e Reggio; Modena, Italy

Key words: chromatin, histone acetylation, histone ubiquitination, KAT3, MNase I ChIP-seq

Post-translational modifications (PTMs) of histones are crucial for transcriptional control, defining positive and negative chromatin territories. A switch of opposing functional significance between acetylation and methylation occurs on many residues. Lysine 120 of H2B is modified by two PTMs: ubiquitination, which is required for further trans-tail H3 methylations and elongation, and acetylation, whose role is less clear. ChIP-Seq with MNase I-treated chromatin indicates that H2BK120ac is present on nucleosomes immediately surrounding the TSS of transcribed or poised units, but not in core promoters. In kinetic ChIP analysis of ER-stress inducible genes, H2BK120ac precedes activation and H2B-ub deposition. Using in vitro acetylation assays, pharmacologic inhibition and RNAi, we established that KAT3 is responsible for H2BK120ac. Interestingly, the global levels of H2B-ub decreased in KAT3-inactivated cells. However, RNF20 recruitment was not impaired by KAT3-inactivation. Our data point at acetylation of Lysine 120 of H2B as an early mark of poised or active state and establish a temporal sequence between acetylation and mono-ubiquitination of this H2B residue.

Introduction

The nucleosome is formed by 146 base pairs of DNA wrapped around core histones. Histone post-translational modifications (PTMs) are associated with accessible chromatin or with heterochromatin, either constitutive or facultative.¹ Some of the PTMs of histones have been characterized at a genome-wide level in several species and it is clear that acetylations are hallmarks of “active” areas of genomes.² Numerous Lysine Acetyl Transferases (KATs) have been discovered as part of large complexes, including KAT2A/B (also known as hGCN5/PCAF) and KAT3 (also known as p300/CBP).³ Acetylations are unstable marks, subject to removal by HDACs. The genome-wide analysis of KATs and HDACs location showed that HDACs are enriched in transcribed units.⁴

A histone PTM that has clearly been associated with gene activity is mono-ubiquitination of Lysine 120 (K123 in yeast) of H2B.⁵⁻⁷ In human cells, the mono-ubiquitination mechanism includes the function of hRAD6 and RNF20/40.⁸ Indeed, the modification of this residue is essential for recruitment of histone methylating activities that act on K4 and K79 of histone H3.^{9,10} However, K120 is also acetylated in bulk histones preparations.¹¹ It is intuitive to assume that these PTMs are mutually exclusive; however, genome-wide analysis suggested that H2BK120ac is part of a “signature” of 17 histone PTMs that mark core promoters of active genes.¹² The well established notion that core promoters are nucleosome-free is at odds with the finding of most of these PTMs in histones positioned in such areas, a fact that could be

rationalized by the relative imprecision of sonicated chromatin-based assays. In addition, using single nucleosome ChIP assays on cell cycle gene promoters, we found H2B-ub in the body of active genes, as expected, whereas acetylation of Lysine 120 was abundant in inactive conditions.¹³ We wished to shed more light on this histone PTM: we used MNase I chromatin¹⁴ to perform ChIP-Seq for H2BK120ac, analyzed an inducible gene system and identified the KAT activity responsible for this modification.

Results

Genomic locations of H2BK120ac. The location of many histone PTMs was mapped by ChIP on Chip and ChIP-Seq experiments using sonicated chromatin. To map H2BK120ac, we performed ChIP-Seq with MNase I-treated chromatin from HCT116 cells, which allows the study of nucleosomes positioning.¹⁴ Reads mapping to single genomic locations were collected and areas in which “peaks” were located analyzed. In parallel, we run two types of controls: input DNA samples derived from MNase I digestion and sonicated chromatin. A total of 18,543 enriched areas were identified out of 31,300 RefSeq genes. Among these regions, areas near the TSS were clearly preferred. **Figure 1A** shows the log ratios of H2BK120ac over MNase I input DNA upstream (-950 from TSS), around the TSS (+50, +100 and +150) and downstream (+950). The “shoulder” of peaks near the TSS is evident. MNase I input reads were plotted against sonicated inputs, showing a bimodal distribution, irrespective of position, with no specific enrichment (**Fig. 1A**, right part).

*Correspondence to: Roberto Mantovani; Email: mantor@unimi.it
Submitted: 02/07/11; Accepted: 03/25/11
DOI: 10.4161/epi.6.5.15623

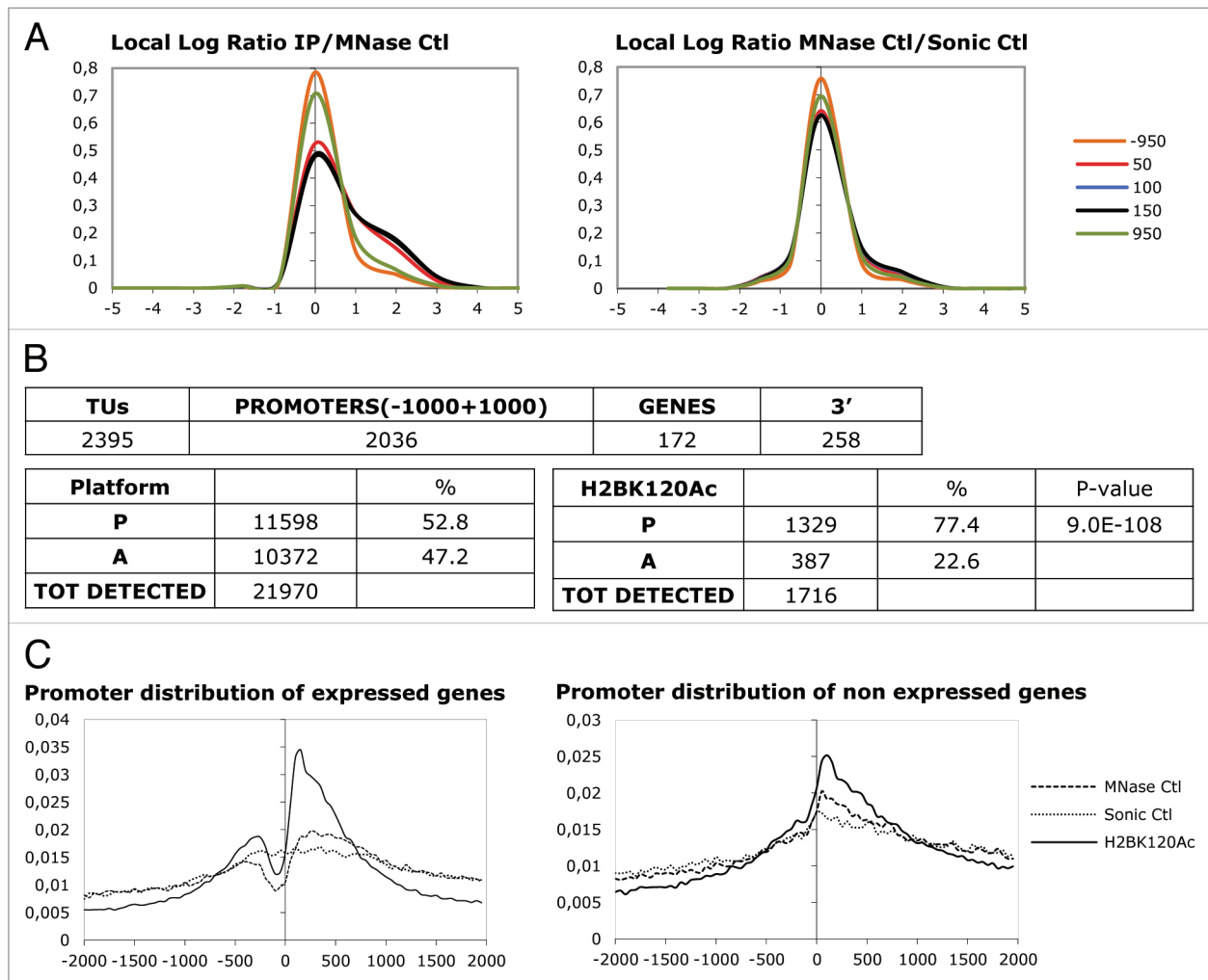


Figure 1. ChIP-Seq analysis of H2BK120ac with MNase I chromatin. (A) Analysis of Log ratios of the peaks relative to the transcriptional start sites (TSS). The different colors refer to the distance from the TSS. In the left part, H2BK120ac IP peaks were plotted against controls represented by MNase I chromatin inputs. In the right part, inputs derived from MNase I and sonicated chromatin were plotted. (B) In the upper part, distribution of high rank H2BK120ac around transcription units (TU) are shown. In the lower parts, Affymetrix expression analysis of high rank H2BK120ac are shown: A (absent) calls refer to non-expressed genes, P (present) calls refer to expressed genes. On the left part, overall distribution of calls is shown; on the right part, H2BK120ac loci are shown. (C) Peaks distribution of H2BK120ac, MNase I and sonicated input control DNAs relative to TSS in expressed (left part) and non-expressed genes (right part).

Next, we extracted the highest scoring H2BK120 peaks in genes and analyzed them for expression patterns, using Affymetrix expression microarrays data (Fig. 1B): P (present) calls, a majority in this type of analysis, are a sign of ongoing transcription, A (absent) calls indicate inactive genes. The skew toward expressed genes was statistically significant. We further analyzed the distribution of H2BK120ac, plotting the peaks as a function of the distance from TSS and separating expressed from non-expressed units (Fig. 1C). The distribution of expressed units showed an enrichment between -200 and -400 (nucleosome -1), a deep dip in the core promoter areas (-200 to +1) and a high peak between +100 and +200 (nucleosome +1). The transcribed areas remained well above the baseline, up to +1,000 (3 or 4 additional nucleosomes). The distribution of control MNase I input DNA showed a very modest dip in the core promoter and a small peak in the +200 to +400 area, while sonicated input DNA was almost completely flat

(Fig. 1C). In non-expressed units, there was a relatively modest peak downstream the TSS (Fig. 1C, right part). Representative loci enriched for H2BK120ac are shown in Supplemental Figure 1. Finally, GO analysis of H2BK120ac genes identified several categories, all with relatively modest enrichments, indicating that the PTM is not unique for a specific category of genes (Sup. Fig. 2). In conclusion, H2BK120 marks nucleosomes immediately upstream and downstream the TSS of expressed units.

To validate the results, we performed independent ChIPs with sonicated chromatin from three cell lines (HCT116, PC3 and U937) on areas at the 5' of 17 genes and, in parallel, analyzed H2B-ub (Fig. 2). In HCT116, most promoters were indeed highly positive for H2BK120ac, with exception of CENPB. H2B-ub was generally low and a detectable enrichment was seen only on EGR1, Jarid1B and TAF4. Similar results were obtained in PC3 and in U937, with exception of PAK2, showing only

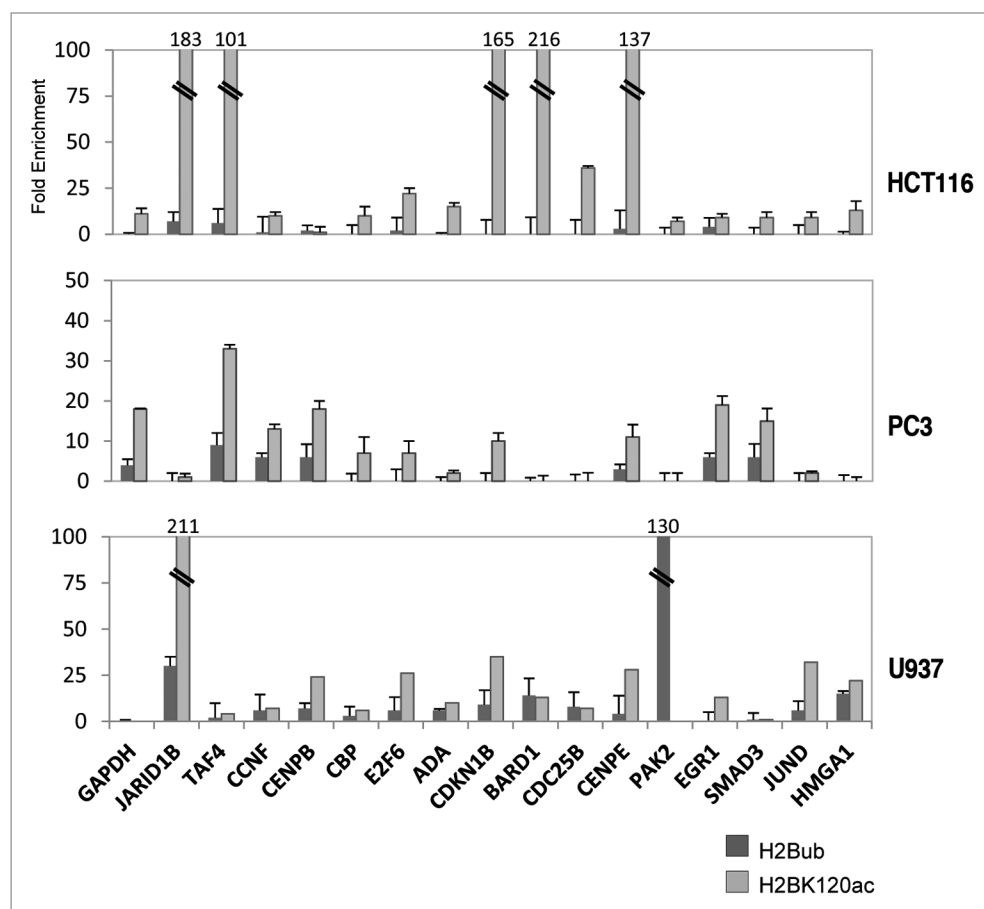


Figure 2. H2BK120 acetylation and mono-ubiquitination in HCT116, PC3 and U937. Analysis of H2BK120 acetylation and mono-ubiquitination on TSS regions of different loci resulting from ChIP-Seq, using sonicated chromatin from HCT116, PC3 and U937 human cell lines. Values are reported as fold enrichment calculated with the following formula: $2^{\Delta Ctx} - 2^{\Delta Ctb}$, where $\Delta Ctx = Ct \text{ input} - Ct \text{ sample}$ and $\Delta Ctb = Ct \text{ input} - Ct \text{ control Ab (Thioredoxin)}$. All values are normalized for the amount of each immunoprecipitated unmodified histone. Error bars represent SD, calculated from four independent experiments.

H2B-ub. In conclusion, the HCT116 ChIP-Seq data were confirmed and extended to other cell lines and chromatin preparations; the coexistence of the two H2BK120 marks suggests a dynamic behavior.

H2BK120 PTMs in the ER-stress inducible system. To dissect the kinetic behavior of the two H2BK120 PTMs, we turned to the ER-stress inducible genes we had previously dissected in reference 15. After treating hepatic HepG2 cells with the ER-stress inducer Thapsigargin, we performed ChIPs with anti-H2BK120ac, anti-H2B-ub and anti-H2B at different time points. Two promoters were analyzed, CHOP/DDIT3 and Herpud1. The former has low basal levels of transcription, as expected and is rapidly induced; the latter is intrinsically more active and slower to be induced (Fig. 3A). We analyzed different regions of the genes. The absence of H2B in the core promoters is expected in poised/active genes (Fig. 3B) and indeed, H2BK120 PTMs were not detected in this area. H2BK120ac basal levels were low but clearly detectable downstream of the TSS, while H2B-ub was negligible. After 1 h induction, H2BK120ac increased substantially in transcribed areas, while H2B-ub remained low. At 4 h, H2B-ub became visible and, at 8 h, H2B-ub further increased, while H2BK120ac substantially

decreased. On Herpud1, H2BK120ac levels were present during basal conditions and decreased upon activation, while H2B-ub enrichment peaked at 8 h (Fig. 3B). As controls, we checked the constitutively active DNA-binding protein SON and the silent tissue-specific AIRE: the former had high levels of H2BK120-ub, but no H2BK120ac; the latter was enriched for none of the two marks (Fig. 3C). In conclusion, inducible ER-stress genes have a basal level of H2BK120ac but no H2B-ub, which increases as acetylation drops.

KAT3 (p300/CBP) is responsible for H2BK120ac. A key question is which KAT is responsible for H2BK120 acetylation. Previous work on KAT2 KO cells ruled out that these enzymes are responsible for this PTM.¹³ We then turned to KAT3A/B. First, we tested whether H2BK120 is targeted by KAT3 in vitro. Recombinant KAT3A catalytic domain was used with four peptides that include the first part of the H2B α C helix. The peptides included two Lysines (K116 and K120) that were either intact (wt) or singularly or dually mutated to Arginine. The KAT3 inhibitor anacardic acid was added to serve as a control for the assay. The data are shown in Figure 4A: the wt peptide was acetylated in vitro, as efficiently as the positive control H4 peptide. Importantly, a K116R peptide was equally well acetylated,

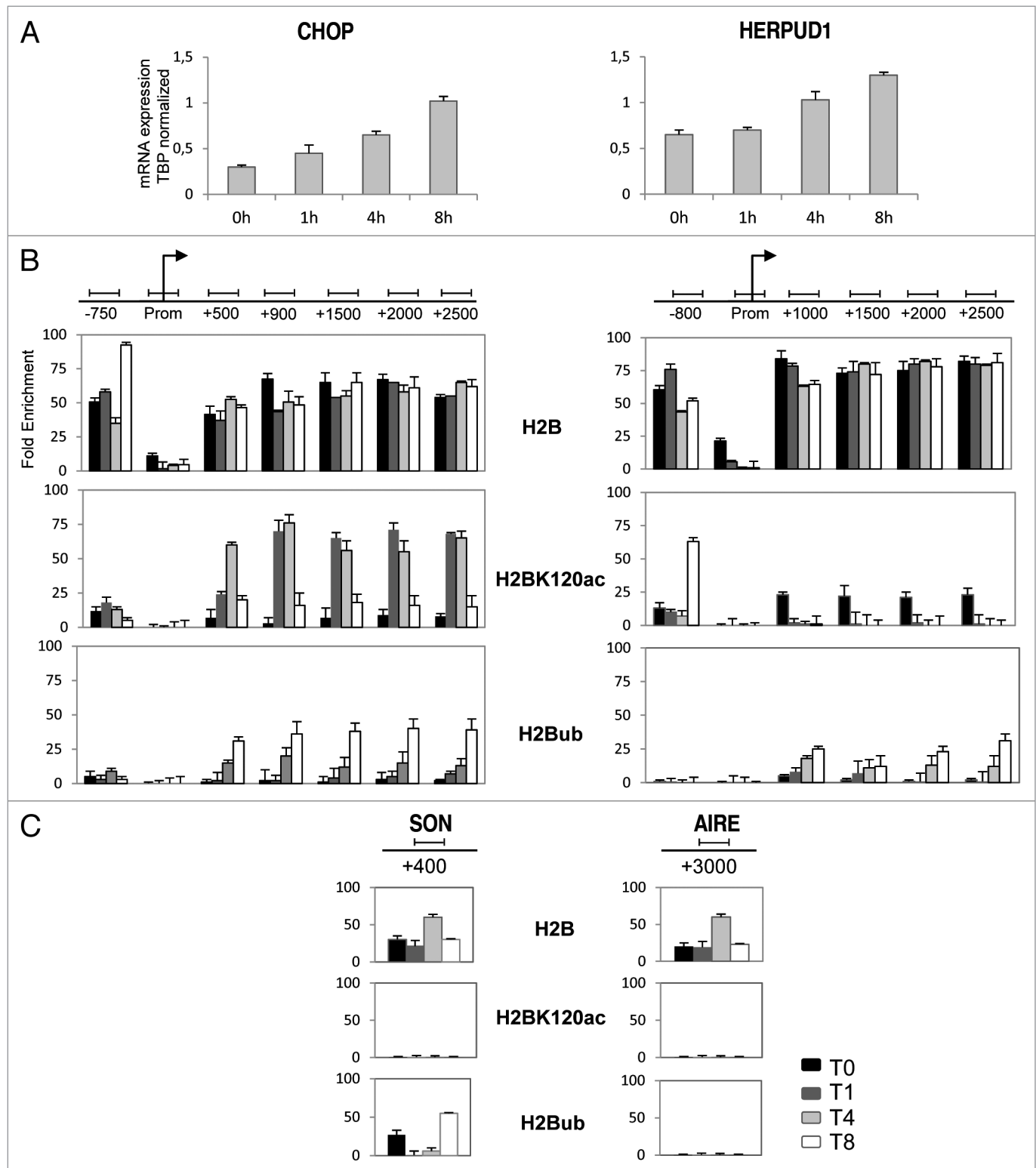


Figure 3. Kinetic deposition of H2BK120 ac and H2BK120-ub on ER-stress inducible promoters. (A) qRT-PCR analysis of the ER-stress CHOP/DDIT3 (left part) and Herpud1 (right part) mRNAs induction in human HepG2 cells after Thapsigargin induction. (B) Kinetic ChIP analysis of H2BK120ac and H2BK120-ub on seven regions of ChOP/DDIT3 (left parts) and six regions of Herpud1 (right parts). In the top parts, the levels of unmodified H2B are shown. The H2BK120 PTMs shown in the lower parts were normalized to the levels of H2B. Analysis of promoter regions were not performed, as residual amount of H2B were scored. (C) Same as (B) on the ubiquitous SON and tissue-specific AIRE promoters. Error bars represent SD, calculated from three independent experiments.

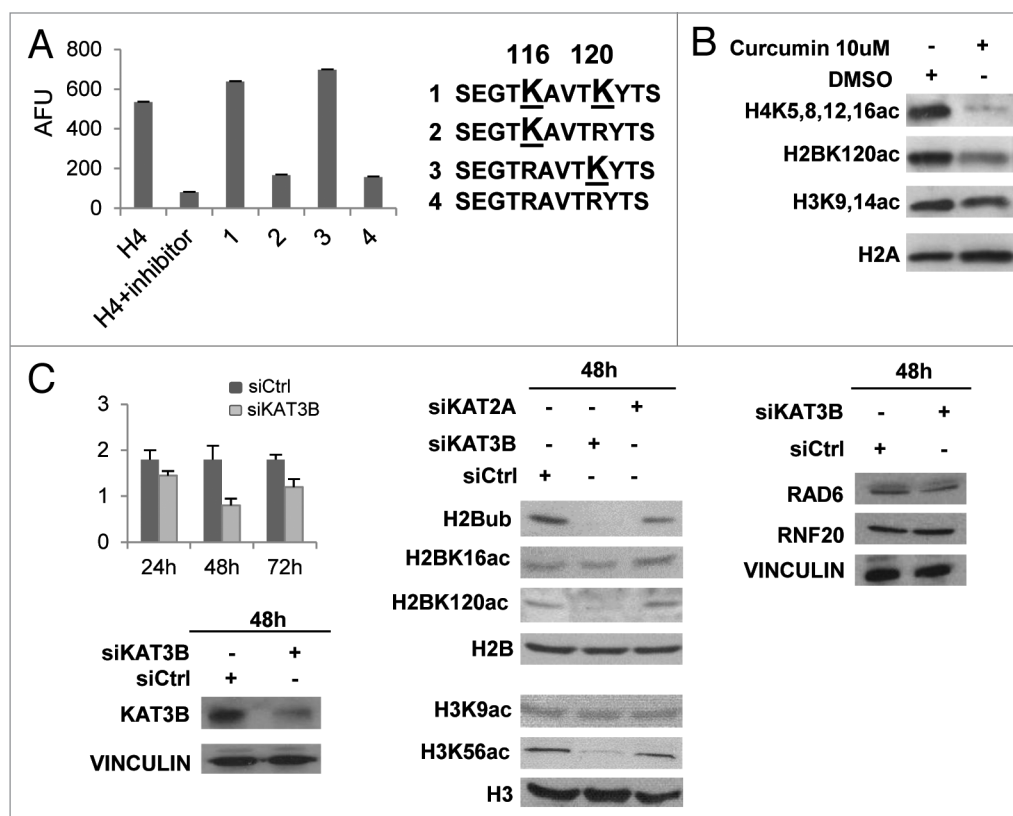


Figure 4. KAT3 is responsible for H2BK120 acetylation. (A) In vitro fluorescent acetylation assay. The assay was performed according to the HAT assay kit (Active Motif) with an H4 peptide (positive control), H4 peptide plus anacardic acid at 15 μ M (HAT inhibitor) and H2B peptides reported in the figure. On the Y axis, Arbitrary Fluorescence Units are plotted. The assay was performed in duplicate. Error bars represent SD, calculated from five independent readings. (B) Western blot analysis of acids extracts of Curcumin-treated HCT116 cells, for the indicated histone PTMs. H2A was used as loading control. (C) PC3 cells transfected with siRNA for KAT3B were controlled for inactivation by qRT-PCR at different time points (left upper part) and by western blot (left lower parts). Vinculin was used as loading control. In the central parts, KAT2A/KAT3B-inactivated PC3 cells (48 h post-transfection) were analyzed for the global levels of different histone PTMs by western blot. H2B and H3 were used as controls. In the right parts, extracts of KAT3B-inactivated PC3 cells (48 h post-transfection) were analyzed for the global levels of RAD6 and RNF20. Vinculin was used as control.

whereas a K120R mutated peptide showed background levels of acetylation, indicating a clear preference of KAT3A for H2BK120. We then wished to confirm these data in vivo. Curcumin is a natural inhibitor of KAT3 enzymatic activities in vitro and in vivo.¹⁶ We treated HCT116 cells with pharmacological concentrations of Curcumin and monitored the global levels of histone PTMs by western blot analysis. **Figure 4B** shows that H4 N-terminal acetylations, known to be imposed by KAT3, were globally reduced, whereas H3K9-14ac was not affected. H2BK120ac was also substantially reduced. To confirm this observation, we inactivated KAT3 in human cells. We first searched for a cell line that would mostly have either KAT3A or KAT3B, and found that prostate carcinoma PC3 cells have predominantly the latter (**Sup. Fig. 3**). We then functionally inactivated KAT3B (and KAT2A/GCN5 as a control) by siRNA and monitored its levels by qRT-PCR, finding a maximal decrease at 48 h post-transfection (**Fig. 4C**, left upper part). Inhibition was confirmed by western blot analysis (**Fig. 4C**, left lower parts). We then checked a number of histone PTMs by western blot (**Fig. 4C** and central parts). Compared to cells transfected with scrambled RNAs or KAT2B siRNAs, KAT3B-inactivated cells showed the expected decrease

in H3K56ac,¹⁷ but not in H3K9ac or H2BK16ac. H2BK120ac was significantly decreased, as well as H2B mono-ubiquitination. Note that the lack of H3K9ac decrease upon KAT2A inhibition was also observed in KO experiments using chicken cells.¹⁸ The global levels of H2B and H3 were not altered. The decrease in H2B-ub could be due to a decrease in the monoubiquitinating enzymes hRAD6 and RNF20; however, western blots using the respective antibodies indicated that their levels were not substantially changed in KAT3B-inactivated cells (**Fig. 4C**, right parts).

To extend these data, we analyzed the loci derived from our ChIP-Seq analysis (see **Fig. 2**) for effects of KAT3A inactivation on the presence of H2BK120 PTMs and RNF20. **Figure 5** shows that the recruitment of KAT3B is vastly decreased upon RNAi and that this correlates with a comparable decrease in H2BK120ac. The levels of H2BK120-ub, which on average were lower, did not change substantially, with the exceptions of CDKN1B, in which they increased, and SMAD3, in which they decreased. Interestingly, the recruitment of RNF20 was robust and moderately affected by KAT3B-inactivation. SMAD3 again showed a more pronounced decrease in RNF20 recruitment, in line with the decrease in acetylation. The high overall levels of

Discussion

The first relevant result regards the switch between acetylation and mono-ubiquitination at K120. Dual histone PTMs have been described on many residues, notably on H3 at Lysines 4, 9, 27, 36, 79. The presence of a switch is an indication of opposing functional roles: H3K9ac and H3K27ac are associated with activity,^{19,20} while trimethylation marks negatively regulated territories. On the other hand, trimethylation of H3K36, and not acetylation, is found in genes with an elongating RNA Polymerase II.¹ Similarly, H3K79 methylation is an active mark,²¹ whereas acetylation is associated to non-transcribing units.¹²

The acetylation/ubiquitination switch is not new, as a plethora of proteins, including transcription factors, are modified by acetylation or sumoylation, as a way to preserve them from poly-ubiquitination-mediated degradation, prolonging their half-life.²² Mono-ubiquitination appears to be a signal with a more immediate regulatory flavor and, in the case of H2B, it is present upstream from histone methylations, being one of the first events that lead to gene activation.⁵ Our previous data suggested that acetylation of H2BK120 might be associated with repression, since it was found on G_1/S gene promoters in G_2/M -arrested cells and on G_2/M genes in G_1/S -enriched cells. A second hypothesis posited that H2BK120ac was a mark of “pre-active” or poised chromatin. Our data support this, as we found H2BK120ac on active genes, in line with the notorious co-activation functions of KAT3, including in the ER-stress system.¹⁵ Interestingly, H2BK120ac appears to precede H2B-ub in RNA Polymerase II elongation and inactivation of KAT3 causes a reduction in the global levels of H2B-ub, suggesting that it is a prerequisite for mono-ubiquitination. However, as many PTMs are affected by KAT3 inactivation, we cannot conclude that it is specifically the lack of H2BK120ac which is causative of this phenomenon. Finally, the dual regulation of H2BK120 should also lead to consider H2AK119-ub, which is associated with Polycomb-mediated transcriptional repression.^{6,23} Indeed, this residue is also acetylated in bulk preparations of histones and a similar switch might be anticipated.

The surprising finding that some of the “repressive” HDACs are bound to expressed genes in T cells⁴ were confirmatory of previous experiments

in yeast showing that they are important to limit histone acetylation in gene promoters, to prevent “spurious” transcription initiating within genes.²⁴ Our data offers a further explanation: HDACs are expected to be involved in the removal of H2BK120ac, among other acetylations, to proceed with mono-ubiquitination.

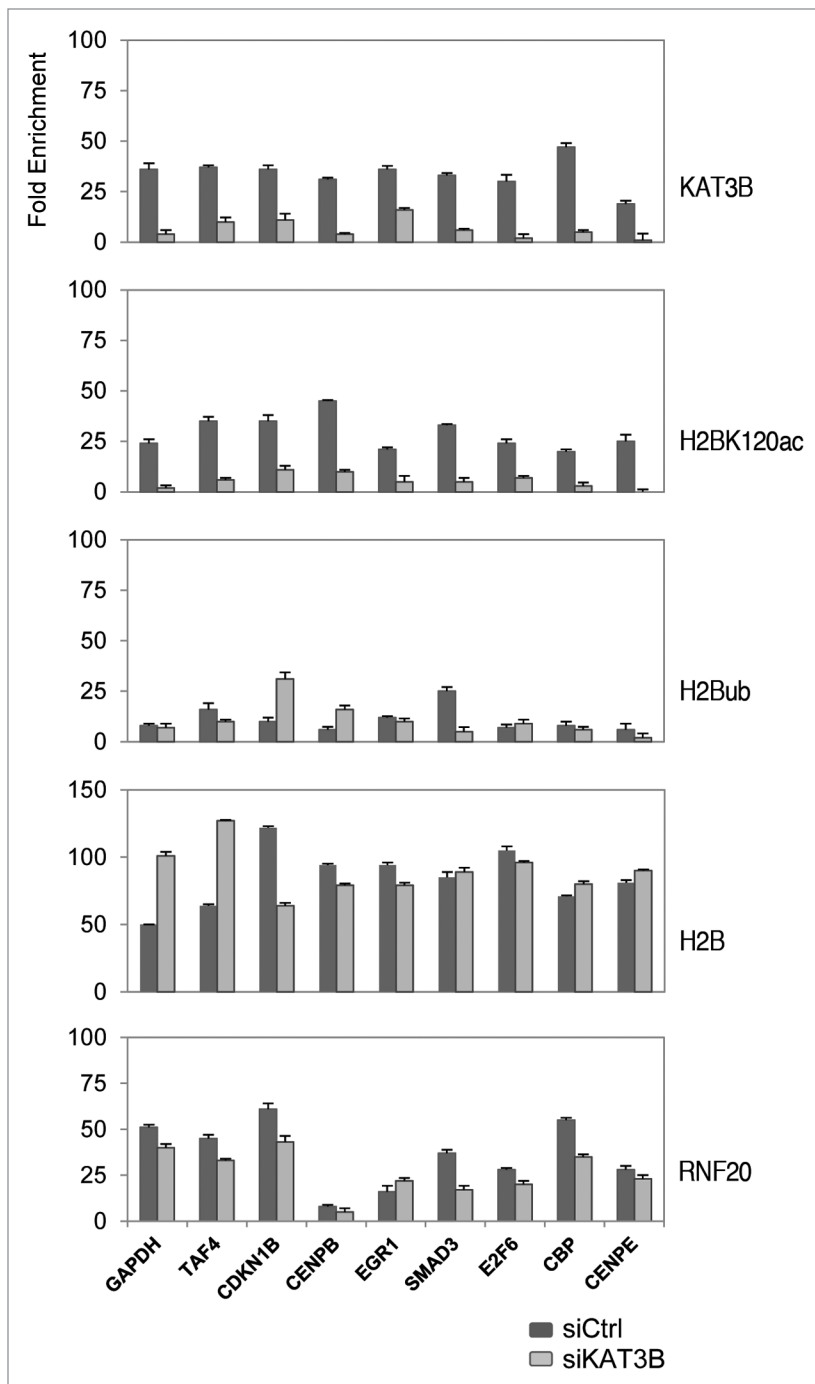


Figure 5. ChIP analysis in KAT3B-inactivated PC3 cells. Analysis of the distribution of KAT3B, H2BK120ac, H2B-ub and RNF20 on TSS regions of the indicated genes in PC3 cells treated with KAT3B and control siRNAs for 48 h, as in Figure 4. ChIPs were performed with the indicated antibodies and analyzed by qPCR with the appropriate primers. Dark grey bars represent data from control cells, the light grey represent data from KAT3B-inactivated. Error bars represent SD, calculated from two independent experiments.

H2B were not significantly affected. Altogether, we conclude that KAT3A/B are responsible for H2BK120 acetylation and, surprisingly, that their inactivation has a negative influence on the levels of H2B mono-ubiquitination, without affecting the H2B mono-ubiquitination apparatus.

In the same framework, we hypothesize that upon removal of the ubiquitin moiety, in nucleosomes neighboring the TSS, acetylation keeps the H2B residue “hot”, ready for subsequent rounds of induction/elongation.

The *in vitro* acetylation data and the decrease of H2BK120ac *in vivo* upon KAT3 inactivation by pharmacologic inhibition and RNAi intervention clearly indicate that KAT3A/B are the major acetylators. Originally identified as transcriptional co-activators, KAT3A/B were shown to acetylate histones, as well many, perhaps most, transcription factors.²⁵ In recent studies, H3K27 and H3K56 were added to the list of KAT3 targets.^{17,20} The latter residue is within the HFD α 1 helix, contacting the phosphate backbone of the nucleosome,²⁶ where acetylation is predicted to disrupt DNA contacts. H2BK120 is in the α C of the HFD, indicating that KAT3 can reach different “inner” areas of the nucleosome. Furthermore, the preference for H2BK120 over the neighboring H2BK116, also acetylated in bulk histones, indicates specificity within this structure.

Finally, we report that the recruitment of E3 RNF20 on a number of promoters is not affected by KAT3 inactivation and consequent decrease in H2BK120ac, indicating that the latter is not used to recruit E3. Interestingly, mono-ubiquitination is not substantially stimulated in the presence of free H2BK120 and RNF20. A trivial explanation would be that the lack of hRAD6, which we could not control for lack of ChIP-grade antibodies, is responsible for this observation; nevertheless, we suspect that this phenomenon might be due to more complex mechanisms, such as a lack of another PTM on histones or on components of the mono-ubiquitination machinery or problems in the recruitment of important cofactors, such as the recently described WAC in reference 27.

The use of heterogeneous cellular populations and the relative lack of precision of ChIPs with sonicated chromatin can potentially blur the interpretation of results on dually regulated marks, speaking in favor of the use of MNase I-treated chromatin (as we used in this work) and of native, non cross-linked chromatin, still to be reported in genome-wide analysis. This should improve our understanding of this enormously complex matter.

Materials and Methods

Cell cultures, chemicals and transfections. HCT116, HepG2, PC3 cell lines were cultured in DMEM medium supplemented with 10% Fetal Calf Serum (FCS), 1% antibiotics (penicillin and streptomycin) and L-glutamine in 5% CO₂; Thapsigargin was used 300 nM, Curcumin at 10 μ M. RNA was extracted at 0, 1, 4 and 8 h using Trizol (Invitrogen). KAT3B knock-down was carried out using Lipofectamine 2000 (Invitrogen) and siRNA.

Acid extracts preparation and western blot analysis. Acid extracts were prepared collecting cells in 5–10 volumes of Lysis Buffer H (10 mM Hepes pH 7.9, 150 mM MgCl₂, 10 mM KCl, 0.5 mM DTT, 1.5 mM PMSF); perchloric acid was added to a final concentration of 0.2 M and cells were kept on ice for 30 min. Extracts were centrifuged 10 min at 11,000 rpm and the supernatants stocked at -80°C. Total extracts were prepared collecting cells in RIPA buffer (50 mM TrisHCl pH 7.4,

150 mM NaCl, 1 mM EDTA, 1% TRITON X-100, 0.5 mM DTT, 1.5 mM PMSF) and centrifuging 20 min at 14,000 rpm. The supernatants were stocked at -80°C. 15 and 10 μ g respectively of total and acid extracts were used in a SDS-PAGE. Proteins were transferred to nitrocellulose and analyzed by western blotting with unmodified H3 (Abcam 1791); unmodified H2B (Abcam 1790); unmodified H2A (Abcam 1764); H3K9,14ac (Upstate); H3K9ac (Active Motif 39137); H2BK16ac (Active Motif 39121); H3K56ac (Upstate 07-677); H4K5,8,12,16ac (Upstate 06-598); H2BK120ac (Active Motif 39119); H2B-ub (Medimabs MM0029); KAT3B/p300 (Santa Cruz sc-585 C20); RAD6 (Abcam 31917); RNF20 (Abcam 32629); Vinculin (Sigma V9131).

***In vitro* acetylation assay.** *In vitro* acetylation assay was performed following instructions provided by Fluorescent HAT Assay Kit (Active Motif, 56100). The purified recombinant p300 catalytic domain was incubated with acetyl-CoA and specific synthetic substrate peptides. The developer solution used reacts with the free sulfhydryl groups on the CoA-SH producing fluorescence, which is read by a fluorometer. Peptides containing the sequence of interest of H2B histone, along with positive and negative controls, were designed and purchased from GenScript. Sequences are reported in Figure 4. For fluorescence reading, a BF1000 Fluorocount was used.

ChIP, ChIP-Seq and data analysis. Single nucleosome ChIP assays were performed as previously described in reference 13, with 3 μ g of the following antibodies: Thioredoxin (Genespin); unmodified H2B (Abcam 1790); H2BK120ac (Active Motif 39119), H2B-ub (Medimabs MM 0029), KAT3A/CBP (sc-369X); KAT3B/p300 (Santa Cruz sc-585 C20); RNF20 (Abcam 32629). The ChIP-PCR primers used for these experiments are reported in reference 12, and in Supplemental Figure 5. Quantitative PCR was performed using SYBR green IQ reagent (Biorad) in the iCycler IQ detection system (Biorad). The relative sample enrichment was calculated with the following formula: $2^{\Delta C_{tix}} - 2^{\Delta C_{tib}}$, where $\Delta C_{tix} = C_{t\text{ input}} - C_{t\text{ sample}}$ and $\Delta C_{tib} = C_{t\text{ input}} - C_{t\text{ control Ab}}$.

Preparation of the samples was based on reference 28, using 2×10^7 cells. After ChIPs, 50 ng of the precipitated DNA were processed with a ChIP-seq single-end sample preparation kit (Illumina), except that the PCR step was performed before gel extraction; the final eluates were sequenced on an Illumina Genome Analyzer II. Sequence reads were mapped against the repeat masked human genome sequence (GRCh37), retrieved from the UCSC genome browser database. Mapping was performed using the Seqmap tool²⁹ (version 1.0.8), allowing up to two substitutions in read matching against the genome. We mapped 1.7×10^7 reads for K120ac IPs, 2.1×10^7 for MNase I and sonicated inputs. Reads distributions near the transcription start site of genes were computed by considering each sequence read as the starting point of a sequence region of 146 bp (nucleosome size). The starting position of each of the reads mapped on the genome was thus shifted by 73 bps downstream (in case of reads mapping on the positive strand) or, vice versa, upstream for reads mapping on the negative strand. The resulting position for each read was used to plot the read distribution. IP versus control enrichment was computed by considering the overall number of

reads uniquely mapping in a given region (selected with respect to the TSS) in both experiments and computing the log-2 of their ratio (using a pseudo-count of one read per region).

Note

Supplemental materials can be found at:
www.landesbioscience.com/journals/epigenetics/article/15623

Acknowledgements

We thank Pekka Ellonen (FIMM, Helsinki FI) for sequencing. This work was supported by AIRC and MIUR-Cofin to R.M.

References

- Berger SL. The complex language of chromatin regulation during transcription. *Nature* 2007; 447:407-12.
- Wang Z, Schones DE, Zhao K. Characterization of human epigenomes. *Curr Opin Genet Dev* 2009; 19:127-34.
- Allis CD, Berger SL, Cote J, Dent S, Jenuwien T, Kouzarides T, et al. New nomenclature for chromatin-modifying enzymes. *Cell* 2007; 131:633-6.
- Wang Z, Zang C, Cui K, Schones DE, Barski A, Peng W, et al. Genome-wide mapping of HATs and HDACs reveals distinct functions in active and inactive genes. *Cell* 2009; 138:1019-31.
- Laribee RN, Fuchs SM, Strahl BD. H2B ubiquitylation in transcriptional control: a FACT-finding mission. *Genes Dev* 2007; 21:737-43.
- Weake VM, Workman JL. Histone ubiquitination: triggering gene activity. *Mol Cell* 2008; 29:653-63.
- Minsky N, Shema E, Field Y, Schuster M, Segal E, Oren M. Monoubiquitinated H2B is associated with the transcribed region of highly expressed genes in human cells. *Nat Cell Biol* 2008; 10:483-8.
- Kim J, Guermah M, McGinty RK, Lee JS, Tang Z, Milne TA, et al. RAD6-Mediated transcription-coupled H2B ubiquitylation directly stimulates H3K4 methylation in human cells. *Cell* 2009; 137:459-71.
- Shilatifard A. Chromatin modifications by methylation and ubiquitination: implications in the regulation of gene expression. *Annu Rev Biochem* 2006; 75:243-69.
- Nakanishi S, Lee JS, Gardner KE, Gardner JM, Takahashi YH, Chandrasekharan MB, et al. Histone H2BK123 monoubiquitination is the critical determinant for H3K4 and H3K79 trimethylation by COMPASS and Dot1. *J Cell Biol* 2009; 186:371-7.
- Cosgrove MS, Boeke JD, Wolberger C. Regulated nucleosome mobility and the histone code. *Nat Struct Mol Biol* 2004; 11:1037-43.
- Wang Z, Zang C, Rosenfeld JA, Schones DE, Barski A, Cuddapah S, et al. Combinatorial patterns of histone acetylations and methylations in the human genome. *Nat Genet* 2008; 40:897-903.
- Gatta R, Mantovani R. Single nucleosome ChIPs identify an extensive switch in cell cycle promoters. *Cell Cycle* 2010; 9:2149-59.
- Gatta R, Mantovani R. NF-Y substitutes H2A-H2B on active cell cycle promoters: recruitment of CoREST-KDM1 and fine-tuning of H3 methylations. *Nucleic Acids Res* 2008; 36:6592-607.
- Donati G, Imbriano C, Mantovani R. Dynamic recruitment of transcription factors and epigenetic changes on the ER stress response gene promoters. *Nucleic Acids Res* 2006; 34:3116-27.
- Balasubramanyam K, Varier RA, Altaf M, Swaminathan V, Siddappa NB, Ranga U, et al. Curcumin, a novel p300/CREB-binding protein-specific inhibitor of acetyltransferase, represses the acetylation of histone/nonhistone proteins and histone acetyltransferase-dependent chromatin transcription. *J Biol Chem* 2004; 279:51163-71.
- Das C, Lucia MS, Hansen KC, Tyler JK. CBP/p300-mediated acetylation of histone H3 on lysine 56. *Nature* 2009; 459:113-7.
- Kikuchi H, Takami Y, Nakayama T. GCN5: a supervisor in all-inclusive control of vertebrate cell cycle progression through transcription regulation of various cell cycle-related genes. *Gene* 2005; 347:83-97.
- Pasini D, Malatesta M, Jung HR, Walfridsson J, Willer A, Olsson L, et al. Characterization of an antagonistic switch between histone H3 lysine 27 methylation and acetylation in the transcriptional regulation of Polycomb group target genes. *Nucleic Acids Res* 2010; 38:4958-69.
- Tie F, Banerjee R, Stratton CA, Prasad-Sinha J, Stepanik V, Zlobin A, et al. CBP-mediated acetylation of histone H3 lysine 27 antagonizes Drosophila Polycomb silencing. *Development* 2009; 136:3131-41.
- Mellor J. Linking the cell cycle to histone modifications: Dot1, G₁/S and cycling K79me2. *Mol Cell* 2009; 35:729-30.
- Sadoul K, Boyault C, Pabion M, Khochbin S. Regulation of protein turnover by acetyltransferases and deacetylases. *Biochimie* 2008; 90:306-12.
- Osley MA. Regulation of histone H2A and H2B ubiquitylation. *Brief Funct. Genomic Proteomic* 2006; 5:179-89.
- Carrozza MJ, Li B, Florens L, Suganuma T, Swanson SK, Lee KK, et al. Histone H3 methylation by Set2 directs deacetylation of coding regions by Rpd3S to suppress spurious intragenic transcription. *Cell* 2005; 123:581-92.
- Chan HM, La Thangue NB. p300/CBP proteins: HATs for transcriptional bridges and scaffolds. *J Cell Sci* 2001; 114:2363-73.
- Luger K. Structure and dynamic behavior of nucleosomes. *Curr Opin Genet Dev* 2004; 13:127-35.
- Zhang F, Yu X. WAC, a functional partner of RNF20/40, regulates histone H2B ubiquitination and gene transcription. *Mol Cell* 2011; 41:384-97.
- Schmidt D, Wilson MD, Spyrou C, Brown GD, Hadfield J, Odom DT. ChIP-seq: using high-throughput sequencing to discover protein-DNA interactions. *Methods* 2009; 48:240-8.
- Jiang H, Wong WH. SeqMap: mapping massive amount of oligonucleotides to the genome. *Bioinformatics* 2008; 24:2395-6.